Ab Initio Treatment of the Chemical Reaction Precursor Complex Cl(^{2}P)−HF. 1. Three-Dimensional Diabatic Potential Energy Surfaces[†]

Anna V. Fishchuk, Paul E. S. Wormer, and Ad van der Avoird*

Theoretical Chemistry, IMM, Radboud University Nijmegen, Toernooiveld 1, 6525 ED Nijmegen, The Netherlands

The three adiabatic potential surfaces of the Cl(^{2}P)−HF complex that correlate with the ^{2}P ground state of the Cl atom were calculated with the ab initio RCCSD(T) method (partially spin-restricted coupled cluster theory including single and double excitations and perturbative correction for the triples). With the aid of a geometry-dependent diabatic mixing angle, calculated by the complete active space self-consistent field (CASSCF) and multireference configuration-interaction (MRCI) methods, these adiabatic potential surfaces were converted to a set of four distinct diabatic potential surfaces required to define the full 3×3 matrix of diabatic potentials. Each of these diabatic potential surfaces was expanded in terms of the appropriate spherical harmonics in the angle θ between the HF bond axis **r** and the Cl−HF intermolecular axis **R**. The dependence of the expansion coefficients on the Cl−HF distance R and the HF bond length r_{HF} was fit to an analytic form. The strongest binding occurs for the hydrogen-bonded linear Cl−HF geometry, with $D_e = 676.5$ cm^{-1} and $R_e = 6.217$ a_0 when $r_{HF} = r_e = 1.7328$ a_0. This binding energy D_e depends strongly on r_{HF}, with larger r_{HF} causing stronger binding. An important contribution to the binding energy is provided by the interaction between the quadrupole moment of the Cl(^{2}P) atom and the dipole of HF. In agreement with this electrostatic picture, the ground state of linear Cl−HF is a 2-fold degenerate electronic Π state. For the linear Cl−FH geometry the states are in opposite order, i.e., the Σ state is lower in energy than the Π state. The following paper in this issue describes full three-dimensional computations of the bound states of the Cl−HF complex, based on the ab initio diabatic potentials of this paper.

1. Introduction

Only recently the importance of the formation of van der Waals complexes in entrance channels of neutral chemical reactions has been fully recognized.[1−5] One of the early examples[1] of this recognition is the study of van der Waals forces in the entrance valley of the Cl + HD reaction, where the van der Waals complex was shown to play a decisive role in the reaction dynamics. As other examples we mention the recent observation of prereactive van der Waals states of the OH−H$_2$ and OH−CO complexes.[2,3] These references emphasize the importance of studying the shallow van der Waals well between reactants, which is a relatively neglected region of reactive potential energy surfaces. See ref 4 for a discussion of how these open-shell prereactive complexes can be investigated by modern spectroscopic methods.

Very recently[6] entrance channel halogen atom−HF complexes were studied by high-resolution infrared laser spectroscopy. The free radical complexes were formed in helium nanodroplets. The authors of this work point out that the elucidation of the structures and energetics of these complexes will require extensive interaction between experiment and theory. Since we fully endorse this statement, we have performed high-level ab initio calculations on the Cl−HF complex. We computed the lowest three adiabatic potential energy surfaces of this complex that correlate with the chlorine atom in its ^{2}P ground state. We also computed a diabatic angle as a function of the three internal coordinates. According to the diabatic model presented in refs

7 and 8 that is summarized below, we obtained from this angle and the three adiabatic surfaces four diabatic potential surfaces from which the full 3×3 matrix of diabatic potentials can be constructed. These ab initio diabatic potential surfaces are used in the subsequent paper[9] in the computation of the rovibrational spectra and structure of the complex. We will see below that the linear geometry Cl−HF has a Π ground state and a first excited Σ state, whereas linear Cl−FH has a Σ ground state and a Π excited state. Deviation from linearity lowers the symmetry from $C_{\infty v}$ to C_s and gives a splitting of the Π states into two states, one of A′ and one of A″ symmetry. A similar observation made by Herzberg and Teller in 1933[10] led Renner to the very first quantum mechanical description of coupling between electronic and vibrational motion.[11]

This paper has the following outline: first we describe how we computed the ground and first excited A′ state by means of the partially spin-restricted coupled-cluster method based on singly and doubly excited states with inclusion of perturbative, noniterative, contributions arising from triply excited states [the RCCSD(T) method].[12] We pay some attention to the counterpoise correction of the interaction energies in these states, because the procedure is not straightforward for the case of a spatially degenerate open-shell monomer. The computation of the energy of the A″ state is discussed. This computation is relatively easy because it regards the lowest state of A″ symmetry. The manner in which the diabatic angle γ is computed from matrix elements of the electronic angular momentum operator L_z is described, and it is shown how a rotation of the two adiabatic A′ states by angle γ leads to two

diabatic states. The third diabatic state is equal to the adiabatic A″ state. The fitting of diabatic potential energy surfaces as a function of two intermolecular Jacobi coordinates and of the H–F bond length r_{HF} is discussed. Finally, results are given and illustrated by some representative cuts through the two-dimensional surfaces.

2. Ab Initio Computations

A Cartesian frame was chosen with as origin the Cl nucleus. The nuclear center of mass of HF ($m_H = 1.0078250321$ u, $m_F = 18.99840320$ u) defines the positive z-axis. It is at a distance R from the Cl nucleus. The vector pointing from H to F lies in the xz-plane of the frame and makes an angle θ with the positive z-axis. The energies were computed on a $14 \times 12 \times 5$-dimensional grid. The following 14 R values were included: $R = 4.5, 5.0, 5.5, 6.0, 6.5, 7.0, 7.5, 8.0, 9.0, 10.0, 12.5, 15.0, 20.0,$ and 25.0 a_0. The θ-grid was a 12 point Gauss–Legendre grid, and the following five H–F distances were taken from ref 13: $r_{HF} = 1.4827, 1.6027, 1.7328, 1.9180,$ and 2.1032 a_0. These points are close to the equilibrium separation and to the classical turning points of the ground and first excited vibrational levels of HF.

All energy calculations were performed by means of the RCCSD(T) method.[12] We used the computer program MOL-PRO[14] in all of the calculations. The atomic orbital basis used was the augmented correlation-consistent polarized-valence triple-ζ basis (aug-cc-pVTZ basis)[15,16] with uncontracted bond functions (exponents sp = 0.9, 0.3, 0.1 and d = 0.6, 0.2) added halfway between the nuclear center of mass of HF and the Cl-atom. The 1s electrons on F and the 1s, 2s, and 2p electrons on Cl were left uncorrelated.

The Cl–HF dimer is of C_s symmetry and possesses three potential energy surfaces that correlate with the ^2P ground state of the free chlorine atom: two of A′ symmetry (correlating with P_x and P_z substates of chlorine) and one of A″ symmetry (correlating with P_y). The MOLPRO RHF program is capable of generating a single determinantal state of the one but lowest energy and the same A′ symmetry as the ground state. This determinant can serve as the reference state for RCCSD(T).

To explain this, we first note that the high-spin-restricted Hartree–Fock (RHF) method, as implemented in MOLPRO, returns highest occupied orbitals of the dimer that are practically pure chlorine 3p-type AOs. The A′ electron configurations are: (cc) $\phi_1(A')\phi_2(A')^2(p_y)^2$, where (cc) stands for the 11 lower lying doubly occupied orbitals, and

$$(\phi_1(A'), \phi_2(A')) = (p_x, p_z)\begin{pmatrix} \cos\gamma_{orb} & \sin\gamma_{orb} \\ -\sin\gamma_{orb} & \cos\gamma_{orb} \end{pmatrix} \quad (1)$$

The orbital energies of the energetically higher, nearly degenerate, AOs $\phi_2(A')$ and p_y vary as a function of θ, and so does the energy of the lower orbital $\phi_1(A')$, with a fairly constant orbital energy difference between $\phi_1(A')$ and $\phi_2(A')$. Notice that the high-spin state (cc) $\phi_1(A')\phi_2(A')^2(p_y)^2$, as computed by MOL-PRO, does not satisfy the Aufbau principle. For $\theta \approx 0°$ the angle γ_{orb} belonging to the lowest A′ state is close to zero, so that $\phi_1 \approx p_x$, $\phi_2 \approx p_z$, and the p_x orbital is singly occupied, while for $\theta \approx 180°$ the angle γ_{orb} is close to 90°, i.e., $\phi_1 \approx p_z$, $\phi_2 \approx p_x$, and the p_z orbital is singly occupied. For $\theta \approx 60°$ the orbitals $\phi_1(A')$ and $\phi_2(A')$ are equally weighted mixtures of p_x and p_z and $\gamma_{orb} \approx 45°$. The lowest RCCSD(T) energy of A′ symmetry is obtained following the standard rules, i.e., with the orbitals from the RHF procedure as input to the RCCSD(T) program. Orbitals for the first excited A′ state are

obtained by swapping $\phi_1(A')$ and $\phi_2(A')$ in the start input to the RHF program, followed by iteration until convergence. The convergent MOs thus obtained enter the RCCSD(T) computation yielding the first excited A′ state of the dimer. Since the RHF iterations do not change the order of the MOs, the excited RCCSD(T) state has a reference configuration in which to a good approximation for $\theta \approx 0°$ the singly occupied AO equals p_z and p_x is doubly occupied, whereas for θ close to 180° p_x is singly occupied and p_z doubly. For $\theta \approx 60°$ the excited-state reference configuration is: (cc) $(p_z + p_x)(p_z - p_x)^2(p_y)^2$, i.e., the orbitals p_x and p_z are mixed with nearly equal weight.

The A″ reference configuration is (cc) $p_y\phi_1(A')^2\phi_2(A')^2$ for all θ, with the p_y orbital singly occupied. The orbitals $\phi_1(A')$ and $\phi_2(A')$ are now nearly degenerate, and still of the form given in eq 1. They are pure p_x and p_z for linear geometries, i.e., $\gamma_{orb} \approx 0°$ for $\theta \approx 0°$ and $\gamma_{orb} \approx 90°$ for $\theta \approx 180°$, and they are mixed with equal weight for $\theta \approx 60°$ (then $\gamma_{orb} \approx 45°$). The p_y orbital is lower by approximately the same amount as the difference in orbital energy of $\phi_1(A')$ and $\phi_2(A')$ in the case of the RHF calculation on the A′ state. Clearly, the A″ electron configuration does not obey the Aufbau principle either. For the linear geometry $\theta = 0°$ (point group $C_{\infty v}$) the lowest RCCSD(T) A′ state is degenerate with the RCCSD(T) A″ state— they are partners in a Π ground state—whereas for $\theta = 180°$ the excited RCCSD(T) A′ state is degenerate with the A″ state; here the Π state is an excited state. The degeneracies are reflected in the orbital energies, which we write briefly as $\epsilon_\alpha(\Gamma)$ with $\alpha = x, y, z$ and $\Gamma = 1A', 2A', A''$. For $\theta = 0°$: $\epsilon_z(A'') = \epsilon_z(1A')$, $\epsilon_x(A'') = \epsilon_y(1A')$, and $\epsilon_y(A'') = \epsilon_x(1A')$. However, for $\theta = 180°$: $\epsilon_z(A'') = \epsilon_z(2A')$, $\epsilon_x(A'') = \epsilon_y(2A')$ and $\epsilon_y(A'') = \epsilon_x(2A')$, so that indeed the A″ configuration (cc) $p_y(p_z)^2(p_x)^2$ has the same energy as the A′ configuration (cc) $p_x(p_z)^2(p_y)^2$ in both cases. As we just saw, the latter configuration yields the A′ ground state for $\theta = 0°$ and the A′ excited state for $\theta = 180°$.

So far we have not discussed the basis set superposition error (BSSE), which usually is taken care of by the counterpoise correction (i.e., subtraction of the sum of the two monomer energies computed in the same dimer AO basis as the dimer energy). The energy of the HF molecule is unambiguously defined, as is the energy of the A″ state of the chlorine atom, but there is a choice for the A′ energy of the free Cl atom. An RHF computation of the A′ state of the free chlorine atom in the dimer basis yields for all angles θ the electronic configuration (cc) $p_z(p_x)^2(p_y)^2$, where p_z is lower in energy than p_x and p_y due to the presence of the hydrogen fluoride basis on the z-axis. The higher two p-orbitals are degenerate. Swapping p_z and p_x in the input of the RHF program followed by iteration changes the total RHF energy by less than 1 cm^{-1}. However, the RCCSD(T) energy of the free Cl atom (in the dimer basis) is much affected by the orbital swap, being 151.6 and 115.0 cm^{-1} lower than the unswapped RCCSD(T) energy for $\theta = 0°$ and 180°, respectively. In our first attempt to correct for the BSSE, we applied the procedure recommended by Kłos et al.[17] according to which the free chlorine p_x and p_z orbitals should be rotated by angles equal to those of the dimer. The results of this procedure were inconsistent, however, in the sense that the degeneracy of the A″ state with one of the A′ states that should occur both for $\theta = 0°$ and $\theta = 180°$ was lifted by the BSSE correction. The failure of this method may be related to the fact that for linear Cl–HF ($\theta = 0°$) the lowest A′ state is degenerate with A″, whereas for linear Cl–FH ($\theta = 180°$) the highest A′ state is degenerate with A″. In Cl–HCl, the system where Kłos et al.[17] tested their method, such a swap does not

Ab Initio Treatment of Cl(^{2}P)−HF

J. Phys. Chem. A, Vol. 110, No. 16, 2006 **5275**

occur. After some experimentation we decided that subtraction of the lowest RCCSD(T) energy of the free chlorine from both A′ dimer energies gives the most consistent results. After this counterpoise correction A′ and A″ remain degenerate Π states for both linear geometries. We reiterate that the lowest RCCSD(T) energy of the free chlorine is obtained by swapping p_x and p_z, obtained from a ground-state RHF calculation, in the input of an RHF plus RCCSD(T) computation. The counterpoise correction for the A″ dimer energy did not pose any problems, we simply subtracted the A″ energy of the Cl-atom [and also the RCCSD(T) energy of the HF molecule, of course].

3. Diabatic Potentials and Analytic Fits

As just discussed, we obtain three adiabatic states $\Psi_1(A′)$, $\Psi_2(A′)$, and $\Psi(A″)$ from the RCCSD(T) computations. They each have as a reference a closed-shell Slater determinant in which a hole is created in the 3p-shell of the chlorine atom. As we saw in section 2 that the hole remains fairly well localized on the Cl atom for all geometries of the complex considered, it is reasonable to assume that the RCCSD(T) states are linear combinations of diabatic states $|P_x\rangle$, $|P_y\rangle$, and $|P_z\rangle$ correlating to the corresponding states of Cl. According to the theory described in refs 7,8 we introduce the diabatic angle γ by writing

$$(\Psi_1(A′), \Psi(A″), \Psi_2(A′)) = (|P_x\rangle, |P_y\rangle, |P_z\rangle)\,\mathbb{R}_y(\gamma), \quad (2)$$

with

$$\mathbb{R}_y(\gamma) \equiv \begin{pmatrix} \cos\gamma & 0 & \sin\gamma \\ 0 & 1 & 0 \\ -\sin\gamma & 0 & \cos\gamma \end{pmatrix}$$

Recalling the expression used by Alexander[7] for the matrix of L_z (the z-component of the chlorine electronic angular momentum operator) in the diabatic basis, we note that the matrix of L_z in the adiabatic basis is (in atomic units $\hbar = 1$)

$$\mathbb{L}_z = \mathbb{R}_y(\gamma)^{\mathrm{T}}\begin{pmatrix} 0 & -i & 0 \\ i & 0 & 0 \\ 0 & 0 & 0 \end{pmatrix}\mathbb{R}_y(\gamma) = \begin{pmatrix} 0 & -i\cos\gamma & 0 \\ i\cos\gamma & 0 & i\sin\gamma \\ 0 & -i\sin\gamma & 0 \end{pmatrix} \quad (3)$$

In the same AO basis as used for the energy computations, we computed $\mathbb{L}_z$ by means of the multireference configuration interaction method (MRCI). This computation was preceded by a complete active space self-consistent field (CASSCF) calculation to generate the natural orbitals that enter the MRCI computations. All configurations obtained by single and double excitations out of the CASSCF wave function were included in the MRCI treatment with internal contraction, giving a total number of about 800 000 configuration state functions. In CASSCF, as well as in MRCI, the 1s orbitals on Cl and F were frozen, as were the 2s and 2p orbitals on the chlorine atom. Initially we froze only the 1s AO on Cl, but then the $2p_z$ orbital on Cl sometimes appeared among the valence orbitals, giving rise to jumps in matrix elements of L_z as a function of geometry. From the MRCI matrix of L_z and eq 3, the angle γ can be obtained. Knowing γ, we compute the diabatic states from the inverse of eq 2.

The BSSE corrected RCCSD(T) adiabatic potentials $V_1(A′)$, $V_2(A′)$, and $V(A″)$, and the MRCI values for $\langle\Psi(A″)|L_z|\Psi_2(A′)\rangle$, $\langle\Psi(A″)|L_z|\Psi_1(A′)\rangle$, were obtained on the grid of R, θ, and r_{HF} mentioned above. The mixing angle γ was determined according to eq 3 from

$$\gamma(R,\theta,r_{\mathrm{HF}}) = \arctan\left[\frac{\langle\Psi(A″)|L_z|\Psi_2(A′)\rangle}{\langle\Psi(A″)|L_z|\Psi_1(A′)\rangle}\right] \quad (4)$$

This is the same expression as used earlier in studies of the nonadiabatic coupling in H_2O[18] and in the Cl−HCl system.[17] The angle γ is used to transform the adiabatic to diabatic energies with the transformation matrix defined in eq 2. A similarity transformation of the diagonal adiabatic matrix gives

$$V_{xx} = V_1(A′)\cos^2\gamma + V_2(A′)\sin^2\gamma$$

$$V_{zz} = V_1(A′)\sin^2\gamma + V_2(A′)\cos^2\gamma \quad (5)$$

$$V_{xz} = [V_2(A′) - V_1(A′)]\sin\gamma\cos\gamma$$

$$V_{yy} = V(A″)$$

It is useful to apply a further transformation, to obtain a spherical basis

$$(|P_x\rangle, |P_y\rangle, |P_z\rangle) = \frac{1}{\sqrt{2}}(|P_{-1}\rangle, |P_0\rangle, |P_1\rangle)\begin{pmatrix} 1 & i & 0 \\ 0 & 0 & \sqrt{2} \\ -1 & i & 0 \end{pmatrix} \quad (6)$$

This gives the four diabatic surfaces

$$V_{0,0} = V_{zz}$$

$$V_{1,1} = V_{-1,-1} = \frac{1}{2}(V_{yy} + V_{xx}) \quad (7)$$

$$V_{1,-1} = \frac{1}{2}(V_{yy} - V_{xx})$$

$$V_{0,1} = -V_{0,-1} = -\frac{\sqrt{2}}{2}V_{xz}$$

To obtain analytic expressions of the diabatic potentials, we made expansions in terms of spherical harmonics $C_\mu^L(\theta,\phi)$, which are normalized such that $C_\mu^L(0,0) = \delta_{\mu,0}$. Recalling that θ is the angle of the HF diatom axis with the z-axis, we write

$$V_{\mu',\mu}(R,\theta,r_{\mathrm{HF}}) = \sum_{L=|\mu'-\mu|}^{L_{\max}} C_{\mu-\mu'}^L(\theta,0)v_{\mu',\mu}^L(R,r_{\mathrm{HF}}) \quad (8)$$

The expansion coefficients were derived using a Gauss-Legendre quadrature on the 12-point ab initio angular grid θ_i with weight w_i:

$$v_{\mu',\mu}^L(R,r_{\mathrm{HF}}) \approx \frac{2L+1}{2}\sum_{i=1}^{12}C_{\mu-\mu'}^L(\theta_i,0)V_{\mu',\mu}(R,\theta_i,r_{\mathrm{HF}})w_i \quad (9)$$

The coefficients $v_{\mu',\mu}^L(R,r_{\mathrm{HF}})$ thus obtained were subsequently fitted as functions of R and r_{HF} by the reproducing kernel Hilbert space (RKHS) method with a two-dimensional kernel for distancelike variables in both dimensions.[19] The R-dependent kernel requires the specification of a parameter m_{RKHS} that describes the large-R behavior of the fitted function. The large-R behavior of the interaction energy in the present system can be described as a series in R^{-n} that starts with $n = 4$. The first two terms of the series contain only spherical harmonics of order $L = 1$ and $L = 2$, respectively. This is because the system consists of an atom in a P state and a heteronuclear diatom in a Σ state. The quadrupole-dipole interaction ($l_A = 2, L = l_B = 1$) is the only term contributing to R^{-4}. Likewise, the quadrupole−quadrupole interaction ($l_A = 2, L = l_B = 2$) is the only long-

TABLE 1: Fit Errors for Near-Linear Geometries, $r_{HF} = r_e$

	$\theta = 0.5°$		$\theta = 179.5°$	
R (a_0)	$V_1(A')$ (cm^{-1})	error (%)	$V_1(A')$ (cm^{-1})	error (%)
4.5	8083.8	−2.63	1549.1	3.06
5.0	1872.3	0.38	215.7	0.69
5.5	−146.0	0.74	−168.3	−0.15
6.0	−644.5	0.14	−236.5	−0.38
6.5	−642.7	−0.02	−211.9	0.02
7.0	−513.7	0.02	−168.4	−0.06
7.5	−381.1	−0.01	−128.9	−0.04
8.0	−276.4	−0.02	−98.2	0.00
9.0	−147.4	0.04	−58.4	0.03
10.0	−83.5	0.02	−35.5	−0.03
12.5	−26.9	0.02	−13.6	−0.05
15.0	−11.5	0.01	−9.11	0.05
20.0	−3.13	−0.03	−3.53	0.16
25.0	−1.17	0.05	−1.54	−0.80

range term that has an R^{-5} dependence. The $l_A = 2$, $l_B = 1$ term was fitted with the RKHS parameter $m_{RKHS} = 3$ and the $l_A = 2$, $l_B = 2$ term was fitted with $m_{RKHS} = 4$. The association of n with a unique value of L stops at $n = 6$. For instance, the $v_{\mu',\mu}^0$ and $v_{\mu',\mu}^2$ coefficients both drop off as R^{-6} since they arise from dispersion (a second-order effect), but also $v_{\mu',\mu}^3$, arising from the quadrupole-octupole ($l_B = 3$) interaction, goes asymptotically as R^{-6}. Therefore, only the $L = 1$ and $L = 2$ coefficients were assumed to have a well-defined R^{-n} behavior and all other coefficients in eq 8 were assumed to have an R^{-6} asymptotic dependence and were fitted accordingly with the RKHS parameter $m_{RKHS} = 5$. For the r_{HF} dependent kernel we chose $m_{RKHS} = 2$. Since the dependence of the coefficients $v_{\mu',\mu}^L(R, r_{HF})$ on r_{HF} is not known analytically, these coefficients were extrapolated linearly in r_{HF} outside the range of the ab initio points. The RKHS parameter n_{RKHS} that defines smoothness of the RKHS functions[19] was chosen to be 2 in all cases.

On the whole the fits were of good quality. For instance, for $R = 5$ a_0 and $r = r_e$ the root-mean-square (RMS) error in $V_{0,0}$ computed on the 12 angular ab initio points is $2.8 \times 10^{-6} E_h$. On this interval the value of $V_{0,0}$ varies between 1.8×10^{-2} and -7.3×10^{-5} E_h. For the same R and r the largest relative error in $V_{1,1}$ is 0.005%. The RMS error in $V_{1,-1} = 6.7 \times 10^{-6}$ E_h with $V_{1,-1}$ varying around -5.0×10^{-4} E_h as a function of θ. The errors in $V_{0,1}$ at the same R and r are somewhat larger, they vary from 1.61% for $\theta \approx 11°$ through 0.09% ($\theta \approx 83°$) to 5.2% for $\theta \approx 169°$. For $R = 7$ a_0 and $r = r_e$ the largest error (2.3%) occurs in $V_{1,-1}$ for $\theta \approx 169°$. For $R = 12.5$ a_0, $r = r_e$, all errors, except two, are less than 0.1%. The two errors larger than 0.1% are in $V_{1,-1}$: 0.5% (for $\theta \approx 11°$) and 3.2% (for $\theta \approx 169°$).

The fit errors discussed so far pertain to points on the ab initio grid. To check the degeneracies of the A' and A'' states for the linear geometries, we performed in the course of this work a number of independent RCCSD(T) calculations very near the linear geometries and yet of C_s symmetry. The expansion errors related to these independent points are given in Table 1. In this table, we find that almost all errors are much less than a percent, so that we may conclude that our fits in terms of associated Legendre functions, cf. eq 8, are very satisfactory.

4. Results and Discussion

In Figure 1, we show one-dimensional cuts through the three adiabatic and diagonal diabatic potentials. The angle $\theta = 0°$ corresponds to the linear hydrogen-bonded structure Cl−HF and $\theta = 180°$ corresponds to linear Cl−FH. The Π state is lowest in energy for $\theta = 0°$, while the Σ state is lowest for $\theta = 180°$,
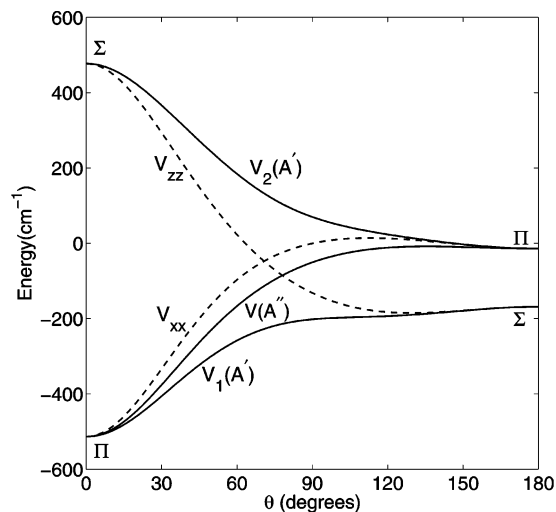

Figure 1. Three adiabatic (full) and diabatic (dashed) curves are shown as a function of θ. $r_{HF} = r_e = 1.7328$ a_0, $R = 7$ a_0. The diabatic curve V_{yy} coincides with the adiabatic curve $V(A'')$, cf. eq 5.

in the entire range of distances R that we considered. For both linear geometries the diabatic energies V_{xx} and V_{zz} coincide with adiabatic energies [with $V_1(A')$ and $V_2(A')$, respectively, for $\theta = 0°$; with $V_2(A')$ and $V_1(A')$, respectively, for 180°]. The curve for the adiabat $V(A'')$, which coincides with the diabat V_{yy}, connects the Π-energies on either side of the plot.

Since upon bending of Cl−HF ($\theta \geq 0°$) the two adiabats show a parabolic behavior, we have here a typical example of the situation studied by Renner[11] 7 decades ago. Pople and Longuet-Higgins[20] refer to this splitting as case 1a and point out that the very first observation of the Renner effect (in the lowest electronic transition of the NH$_2$ radical[21]) must be explained by a different splitting pattern. The adiabatic potentials do not cross, of course, because the corresponding states diagonalize the electronic Hamiltonian, but the diabats V_{xx} and V_{zz} do cross (at $\theta \approx 60°$). We discussed in section 2 that the Cl $3p_x$ and $3p_z$ orbitals mix as a function of θ and it is no coincidence that around the same angle ($\theta \approx 60°$) the orbitals are mixed with equal weight. Had we taken the diabatic angle to be the orbital mixing angle γ_{orb}, we would have found the crossing of the diabats at about the same θ.

For the angle $\theta = 180°$ the Σ state lies lower than the Π state, $V_{zz} < V_{xx}$, while for $\theta = 0°$: $V_{zz} > V_{xx}$. This flipping in the state order follows from the fact that the $3p_x$ and $3p_z$ orbital have swapped places in going from linear Cl−HF to linear Cl−FH, as we discussed above. The relative positions of the orbital and total binding energies can be understood by considering the dipole of HF. It points from F$^{\delta-}$ to H$^{\delta+}$. The chlorine atom has a hole in an argon-like 3p shell and we remember that a hole can be thought of as a positively charged particle. The hole is attracted by the negative charge on the F atom and therefore will prefer to be in $3p_z$ (a σ-orbital pointing toward the F atom), when this atom is closest to Cl. This implies that in Cl−FH the state of Σ symmetry has the lowest energy. On the other hand, in Cl−HF the chlorine hole tries to avoid the positively charged hydrogen atom and will be in a π orbital, leading to a lower Π state for $\theta = 0°$.

In Figures 2−4, the adiabatic potentials $V_1(A')$, $V_2(A')$, and $V(A'')$ are shown as a function of R and θ for fixed r_{HF}. The absolute minimum in the lowest adiabat $V_1(A')$ for $r_{HF} = r_e = 1.7328$ a_0 occurs for $R = 6.217$ a_0, $\theta = 0°$. The well depth is $D_e = 676.5$ cm^{-1}. This minimum, being 2-fold degenerate, coincides with the global minimum in $V(A'')$.

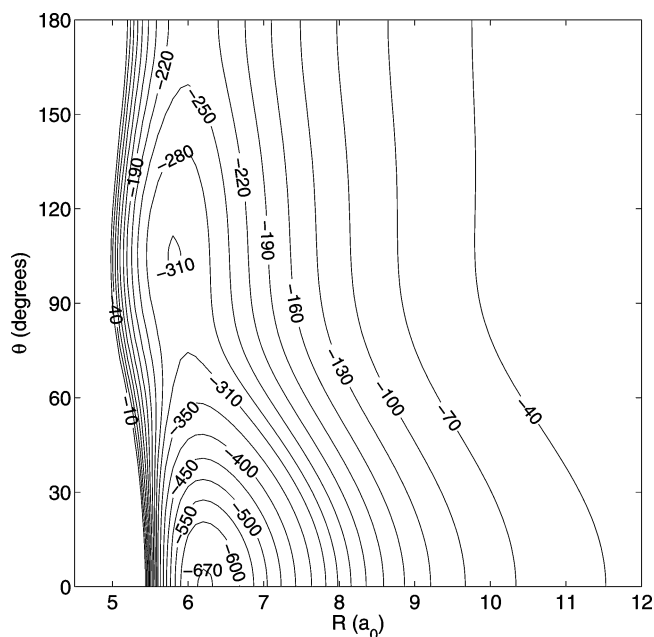Ab Initio Treatment of Cl(^{2}P)−HF

J. Phys. Chem. A, Vol. 110, No. 16, 2006 **5277**

Figure 2. Adiabatic surface $V_1(A')$ as a function of R and θ, for $r_{HF} = r_e = 1.7328\ a_0$.

Figure 4. Adiabatic surface $V(A'')$ as a function of R and θ, for $r_{HF} = r_e = 1.7328\ a_0$.

Figure 3. Adiabatic surface $V_2(A')$ as a function of R and θ, for $r_{HF} = r_e = 1.7328\ a_0$.
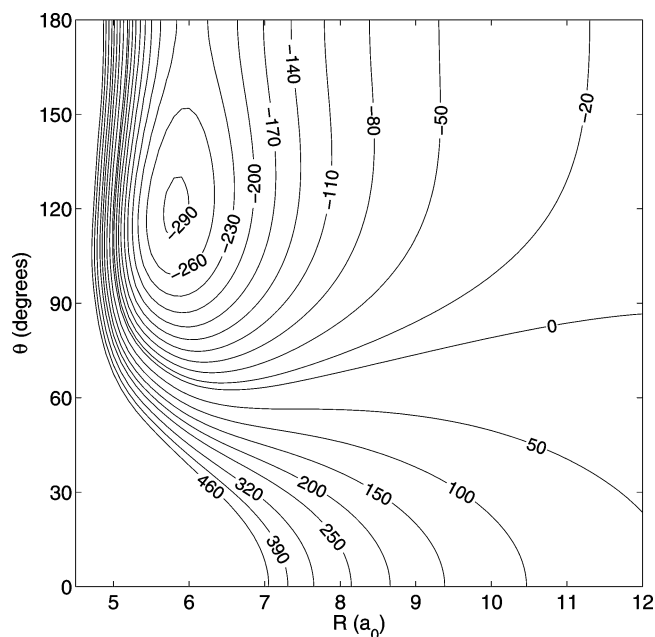
Figure 5. Diabatic surface $V_{0,0}$ as a function of R and θ, for $r_{HF} = r_e = 1.7328\ a_0$.

Figures 5−8 show the diabatic potentials $V_{0,0}$, $V_{1,1}$, $V_{1,-1}$, and $V_{0,1}$, respectively, as a function of R and θ for fixed $r_{HF} = r_e$. The absolute minimum with $D_e = 676.5$ cm^{-1} in the adiabatic potentials $V_1(A')$ and $V(A'')$ for the linear Cl−HF geometry is due to a similar minimum in the diabatic potential $V_{1,1} = V_{-1,-1}$ that corresponds to the Π state. The diabatic potential $V_{0,0}$ for the Σ state shows a much shallower minimum of depth 295.3 cm^{-1} for $\theta = 120°$ and $R = 5.8\ a_0$. The latter minimum is reflected in the lowest adiabatic potential $V_1(A')$ in Figure 2 as a shallow local minimum. The off-diagonal diabatic potential $V_{1,-1}$ is relatively small, which indicates according to eq (7) that the diabatic surfaces V_{xx} and V_{yy} are nearly equal. These surfaces V_{xx} and V_{yy} correspond to the electron hole on the Cl atom being in a p$_x$ or p$_y$ orbital, respectively. The fact that they are so similar even for $\theta \approx 90°$, i.e., when the HF axis is nearly perpendicular to the intermolecular Cl−HF axis, is somewhat
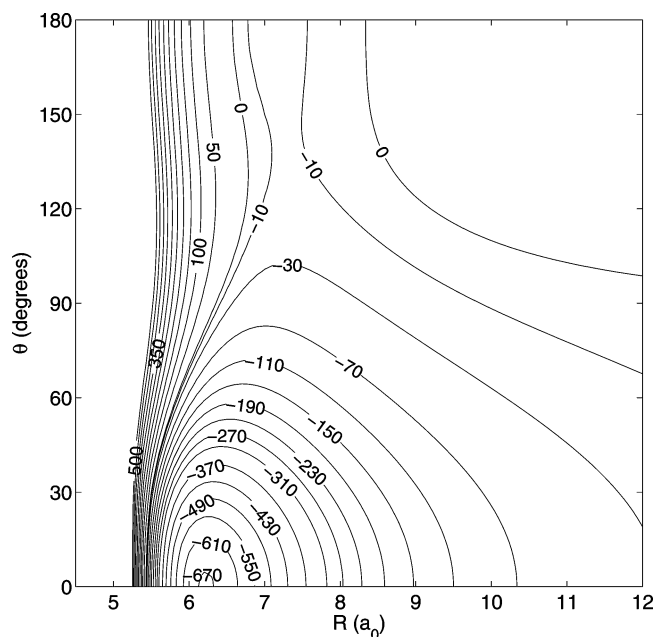
surprising. The potential $V_{1,-1}$ is always negative, which implies that V_{xx} is larger than V_{yy}; cf. Figure 1. The off-diagonal diabatic potential $V_{0,1}$ is larger in absolute value and changes sign for a θ value of about 120° for small R. The value of θ where this sign change occurs increases with R; for $R > 7\ a_0$, $V_{0,1}$ is negative for all values of θ.

The potential surfaces for other values of r_{HF} are qualitatively similar, but the depth of the well in $V_1(A')$ and $V(A'')$, which corresponds to the well in $V_{1,1}$, increases strongly with increasing r_{HF}; see Table 2. As we show in ref 9, this plays an important role in the explanation of the large red shift of the HF stretch vibration induced by the interaction with the Cl atom that was observed experimentally.[6]

Our results may be compared with the results of the ab initio calculations by Merritt et al.[6] for the linear geometries Cl−HF and Cl−FH. They find the strongest binding for Cl−HF, as we
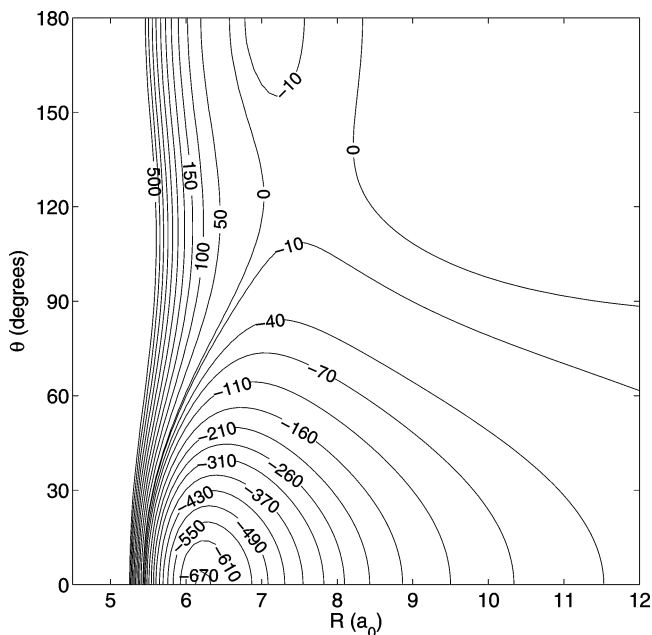
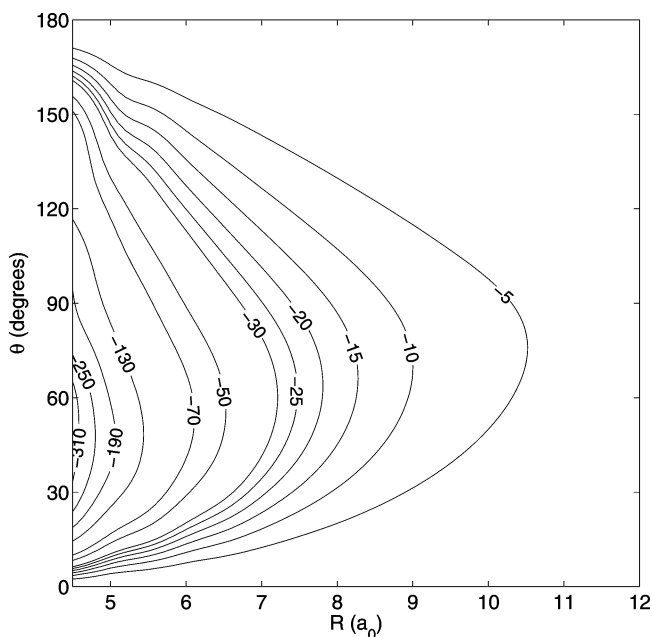**Figure 6.** Diabatic surface $V_{1,1}$ as a function of R and θ, for $r_{HF} = r_e$ = 1.7328 a_0.

Figure 8. Diabatic surface $V_{0,1}$ as a function of R and θ, for $r_{HF} = r_e$ = 1.7328 a_0.

TABLE 2: Dependence of the Well Depth D_e in $V_{1,1}$ and the Equilibrium Distance R_e on r_{HF}

r_{HF} (a_0)	R_e (a_0)	D_e (cm^{-1})
1.4827	6.2356	−513.95
1.6027	6.2350	−579.52
1.7328	6.2166	−676.50
1.9180	6.1558	−861.14
2.1032	6.0665	−1129.79

hydrogen bonded X−HX structure is about equally deep for Br−HF as for Cl−HF, but considerably shallower for the other systems. The local minimum in $V_1(A')$ at the T-shaped geometry is only very shallow for Cl−HF. For Cl−HCl, it is the global minimum, and also for Br−HF, F−HF, and Br−HBr, it is a more pronounced local minimum than for Cl−HF. The observation that the Π state is lower than the Σ state at the linear X−HX structure while the Σ state is lower at the linear X−XH structure, see Figure 1, holds also for the semiempirical potentials of F−HF and Br−HF, but not for the ab initio potential of Cl−HCl, for example.

5. Conclusion

We described the ab initio calculation of the adiabatic potential surfaces of the Cl(^{2}P)−HF complex that correlate with the (in the absence of spin−orbit coupling) 3-fold degenerate ^{2}P ground state of the Cl atom. These potential surfaces are converted with the aid of a geometry-dependent diabatic mixing angle, also calculated ab initio, to a set of four distinct diabatic potential surfaces required to define the full 3 × 3 matrix of diabatic potentials. Each of these diabatic surfaces was expanded in terms of the appropriate spherical harmonics in the atom−diatom Jacobi angle θ. The dependence of the expansion coefficients on the Cl−HF distance R and the HF bond length r_{HF} was fit to an analytic form. The resulting potentials were discussed and are used in ref 9 in full three-dimensional computations of the bound states of the Cl−HF complex.

Figure 7. Diabatic surface $V_{1,-1}$ as a function of R and θ, for $r_{HF} = r_e$ = 1.7328 a_0.

do, with D_e = 672 and 676 cm^{-1} at the UMP2 and UCCSD(T) levels, respectively. This agrees very well with our value of D_e = 676.5 cm^{-1} from RCCSD(T) calculations. For linear Cl−FH they find a binding energy of only 20 cm^{-1}, whereas we obtain a much larger value: 237.4 cm^{-1}. Our value corresponds to the lowest state of A′ symmetry, however, and their value corresponds to the state of A″ symmetry[22] (which gives the strongest binding for linear Cl−HF, where it is degenerate with the lowest A′ state). Our value for the well depth of linear Cl−FH in the A″ state is 14.3 cm^{-1}, in fairly good agreement with their value of 20 cm^{-1}.

We may also compare our potential surfaces for Cl−HF with the ab initio potentials of Kłos et al. for the analogous systems Cl−HCl,[17,23] F−HF, and Br−HBr[24] and with the semiempirical F−HF and Br−HF potentials of Meuwly and Hutson.[25,26] The minimum in the lowest adiabatic potential $V_1(A')$ at the linear
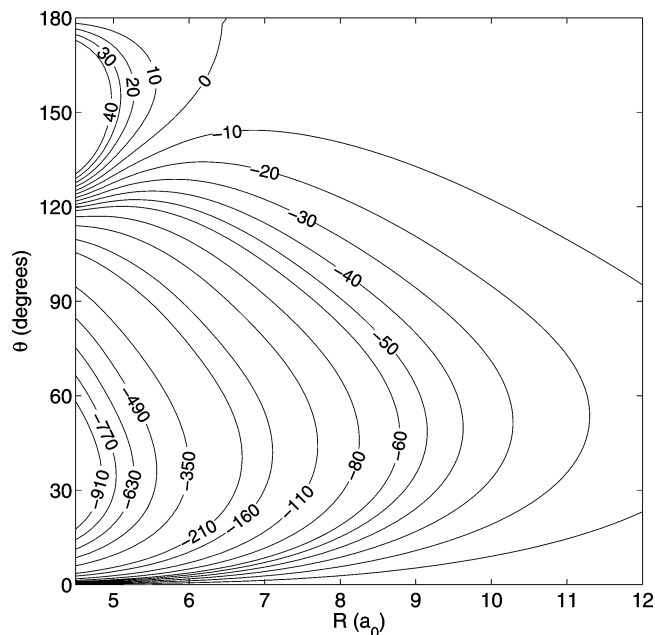
Ab Initio Treatment of Cl(^{2}P)−HF

J. Phys. Chem. A, Vol. 110, No. 16, 2006 **5279**

References and Notes

(1) Skouteris, D.; Manolopoulos, D. E.; Bian, W.; Werner, H.-J.; Lai, L.-H.; Liu, K. *Science* **1999**, *286*, 1713−1716.

(2) Wheeler, M. D.; Anderson, D. T.; Lester, M. I. *Int. Rev. Phys. Chem.* **2000**, *19*, 501.

(3) Lester, M. I.; Pond, B. V.; Marshall, M. D.; Anderson, D. T.; Harding, L. B.; Wagner, A. F. *Faraday Discuss. Chem. Soc.* **2001**, *118*, 373.

(4) Neumark, D. M. *Phys. Chem. Commun.* **2002**, *5*, 76.

(5) Xie, T.; Wang, D.; Bowman, J. M.; Manolopoulos, D. E. *J. Chem. Phys.* **2002**, *116*, 7461.

(6) Merritt, J. M.; Küpper, J.; Miller, R. E. *Phys. Chem. Chem. Phys.* **2005**, *7*, 67−78.

(7) Alexander, M. H. *J. Chem. Phys.* **1993**, *99*, 6014.

(8) Zeimen, W. B.; Kłos, J. A.; Groenenboom, G. C.; van der Avoird, A. *J. Chem. Phys.* **2003**, *118*, 7340−7352.

(9) Fishchuk, A. V.; Groenenboom, G. C.; van der Avoird, A. *J. Phys. Chem. A* **2005**, *110*, 5280.

(10) Herzberg, G.; Teller, E. *Z. Phys. Chem. B* **1933**, *21*, 410.

(11) Renner, R. *Z. Phys.* **1934**, *92*, 172.

(12) Knowles, P. J.; Hampel, C.; Werner, H.-J. *J. Chem. Phys.* **1993**, *99*, 5219−5227.

(13) Jeziorska, M.; Jankowski, P.; Szalewicz, K.; Jeziorski, B. *J. Chem. Phys.* **2000**, *113*, 2957.

(14) MOLPRO is a package of ab initio programs written by H.-J. Werner and P. J. Knowles, with contributions from J. Almlöf, R. D. Amos, A. Berning, D. L. Cooper, M. J. O. Deegan, A. J. Dobbyn, F. Eckert, S. T. Elbert, C. Hampel, R. Lindh, A. W. Lloyd, W. Meyer, A. Nicklaβ, K. Peterson, R. Pitzer, A. J. Stone, P. R. Taylor, M. E. Mura, P. Pulay, M. Schütz, H. Stoll and T. Thorsteinsson.

(15) Kendall, R. A.; Dunning, T. H.; Harrison, R. J. *J. Chem. Phys.* **1992**, *96*, 6796.

(16) Woon, D. E.; Dunning, T. H., Jr. *J. Chem. Phys.* **1993**, *98*, 1358−1371.

(17) Kłos, J.; Chałasiński, G.; Szcześniak, M. M.; Werner, H.-J. *J. Chem. Phys.* **2001**, *115*, 3085.

(18) Dobbyn, A. J.; Knowles, P. J. *Mol. Phys.* **1997**, *91*, 1107.

(19) Ho, T.-S.; Rabitz, H. *J. Chem. Phys.* **1996**, *104*, 2584.

(20) Pople, J. A.; Longuet-Higgins, H. C. *Mol. Phys.* **1958**, *1*, 372−383.

(21) Dressler, K.; Ramsay, D. A. *Philos. Trans. R. Soc. London* **1959**, *251A*, 553.

(22) Miller, R. E. Private communication, **2005.** In ref 6, the A′ or A″ symmetry was not specified.

(23) Zeimen, W. B.; Kłos, J. A.; Groenenboom, G. C.; van der Avoird, A. *J. Phys. Chem. A* **2003**, *107*, 5110−5121.

(24) Kłos, J.; Szcześniak, M. M.; Chałasiński, G. *Int. Rev. Phys. Chem.* **2004**, *23*, 541.

(25) Meuwly, M.; Hutson, J. M. *J. Chem. Phys.* **2000**, *112*, 592.

(26) Meuwly, M.; Hutson, J. M. *J. Chem. Phys.* **2003**, *119*, 8873.